Ion Clustering in Styrene-Based Ionomers: Calorimetric and Gravimetric Hydration Studies and Effect of Ion Concentration and Thermal History

M. ESCOUBES, *Université Claude Bernard, 69621 Villeurbanne, France*, M. PINERI, *Centre d'Etudes Nucléaires de Grenoble, 38041 Grenoble Cédex, France*, and S. GAUTHIER and A. EISENBERG, *McGill University, Department of Chemistry, Montreal, Quebec H3A 2K6, Canada*

Synopsis

The water sorption behavior of styrene–methacrylic acid copolymers and of their sodium salts has been studied as a function of concentration of ionic groups and nature of the sample. The influence of thermal history has also been examined. The salt forms of the copolymers were found to have a greater hydration capacity than the acids, the hydration capacity increasing with ion content for the salts. The hydration energy of the acid forms was found to be in the vicinity of the liquefaction energy of water whereas the energy for the salt forms became much lower than that value, with increasing water content. This decrease in energy has been attributed to a rearrangement of the cluster structure to accommodate more water molecules.

INTRODUCTION

In the last few years, the physical properties of ion-containing polymers have been the subject of a number of theoretical and experimental studies.[1–3] The reason for the interest in these materials lies in the fact that significant changes in the structure and properties occur when ions are introduced into polymers, primarily due to the coulombic interactions between the ions.

The properties of several ionomer families have been explored in considerable detail. These include the ethylene ionomers,[4–8] the styrene ionomers,[9–16] as well as a group of ionomers based on materials of low T_g such as the dienes,[17–19] the ethylene–propylene copolymers,[20,21] the ethyl acrylates,[22] and the polypentenamers.[23,24] More recently, the perfluorinated ionomer membranes (Nafion® and others) have received considerable attention.[25] This is by no means an exhaustive list.

Specifically in regard to the styrene ionomers, at low ion concentrations one observes a systematic increase in the glass transition with ion-content (~3.5°C/mol % ions), a broadening of the transition region in the viscoelastic properties, as well as the appearance of a secondary pseudorubbery inflection in the modulus, reflecting extensive ion aggregation. At ca. 6 mol % ions, these changes are accelerated. Beyond this point, time–temperature superposition in stress–relaxation fails, and a new dynamic mechanical peak appears which increases in intensity and shifts to higher temperatures with increasing ion content. A small-angle X-ray peak also becomes evident.[26] These phenomena are related to the presence of two types of ionic aggregates, clusters and multiplets, the existence of which has been confirmed by dielectric[27] and Raman[28]

Journal of Applied Polymer Science, Vol. 29, 1249–1266 (1984)
 CCC 0021-8995/84/041249-18$04.00

studies. The multiplets act as simple time and temperature dependent cross-links, whereas the clusters are larger aggregates containing a considerable amount of chain backbone material. These aggregates give rise to the small-angle X-ray scattering behavior which has been observed.

In styrene–methacrylic acid copolymers, the acid forms do not show phase separation, and no effect associated with the presence of multiplets has been observed. The acid groups are thus probably dispersed as dimers. Another distinguishing characteristic between acid and salt forms is the much greater hydration capacity of the salts, but no precise equilibrium values have as yet been obtained in the one very preliminary study of hydration which has been published to date on the styrene ionomers.[12]

In addition to the studies now underway to characterize structure–properties relations in styrene ionomers, several studies have been undertaken to elucidate the nature of the aggregates. These include small-angle-neutron scattering[29] as well as studies of the hydration behavior which is the subject of the present article. This study is specifically aimed at the elucidation of the water sorption behavior as a function of the concentration of ions, especially in the vicinity of the critical concentration (6 mol %), as well as the influence of the thermal history of the sample. Furthermore, the effect of particle size or dimension of the adsorbent will be explored in that, on the one hand, powdery freeze-dried samples will be investigated in one set of measurement and the results compared with studies on ca. 0.3 mm discs. The latter results will be further compared with results of the preliminary study of water absorption in 1 mm thick samples.[12]

The techniques to be utilized in this study involve coupled microgravimetric–microcalorimetric measurements which were used primarily for powdery (freeze-dried) samples, as well as regular gravimetric techniques for water sorption by bulk samples.

EXPERIMENTAL

Coupled Microgravimetric and Microcalorimetric Measurements

In this phase of the work, the sorption was studied on a previously described instrument[30] which employed a recording electronic microbalance coupled to a differential microcalorimeter employing thermocouples. The hydration of the copolymers was followed both thermally and gravimetrically.

The experimental procedure is as follows: Before sorption, the two chambers are connected to a vacuum installation which permits the degassing of the two samples *in situ* at 10^{-4} torr. It is also possible to perform thermal treatments *in situ*, at different rates and temperatures, under vacuum or under a controlled atmosphere. During sorption, the desired vapor pressure is obtained and maintained by connecting the two chambers to an evaporator filled with water, which can be regulated between −80°C and 20°C ± 0.2°C. The two samples are then thermostated at the same temperature. Any deviation between the two interior thermocouples (situated as close to the samples as possible) is recorded. Even when such precautions are taken, however, it seems difficult to work at pressures approaching the saturation pressure if the isotherm is increasing exponentially, since the slightest deviation in temperature causes major differences between the sorption of the two specimens. For each pressure in-

crement, the weight variation and the thermal response are recorded simultaneously on the two channels of a SEFRAM recorder. It is therefore possible to calculate a molar interaction energy by taking a simple ratio of the normalized outputs representing the weight and energy changes.

The coupling, as described above, thus permits the simultaneous recording of three types of measurements, namely, the determination of sorption–desorption isotherms, the kinetic analysis of the data during each pressure increment, and the study of the molar energy of interaction during water sorption. The sensitivity of the MTB 10.8 SEFRAM microbalance is better than 1 μg. The sensing element of the microcalorimeter traces the thermal response on the recorder with a sensitivity of 5 μV/mW. The detection limit (stability of the base line in the isotherm) is about 80 μW, corresponding to a 1 mm deviation if the recorder is set at 100 μV full scale. It can be assumed that signals greater than 800 μW are measurable under good conditions.

Analysis of the Calorimetric Data

For the study described here, the experimental value of the molar interaction energy must be transformed into thermodynamic values. The procedure described above corresponds to an isothermal microcalorimetry experiment in an open system,[30-32] which is characterized by the following features:

(a) For an infinitesimal transformation, the amount of heat dQ, normalized to 1 mol, may be expressed from the molar internal energies of the gas, E_g, and of the sorbed phase, E_a, as:

$$\frac{dQ}{dn_a} = E_a - E_g + n_a \frac{dE_a}{dn_a} - RT$$

This equation corresponds exactly to the thermodynamic expression for the isosteric heat calculated from isotherms using the Clausius–Clapeyron equation.

(b) In practice, the integrated expression should be used during a pressure increment. It can be shown that the calorimetric value $\Delta Q/\Delta n_a$ then corresponds to the average internal energy variation of 1 mol going from the gaseous to the sorbed phase during this increment; it is not an average involving all the material absorbed to that point. This calorimetric measurement is therefore very useful for the detection of changes in the nature of the interaction. It permits a reliable determination of the energy profile of the sorption.

(c) The adsorbed phase, as defined by the thermodyanmic values, is in reality valid for the adsorbate and adsorbent together. If the solid is not inert, the calorimetric measurement will also reflect the variation in its internal energy. This is particularly important in solvent–polymer interactions where possible diffusion or dissolution may cause major modifications of the solid phase.

Direct Calorimetric Measurements

Some of the advantages of direct calorimetric measurements are that an experimental measure of the interaction may be obtained, the existence of several successive levels of interaction may be detected and their relative importance during the sorption may be evaluated.[33] This type of measurement is particu-

larly important because it is the only one which permits an evaluation of the amounts of water that may be considered as energetically bound. At first, it seems unlikely that water should be strongly bound to the polymer.[34] Even in hydrophilic polymers, hydrogen bonding with hydroxyl, amide, or carbonyl functional groups is relatively weak, and sometimes lower than the bonding between water molecules in the liquid phase. The concept of bonded water should thus be used with some caution, especially when it is deduced from indirect measurements.[35] The enthalpy values are often calculated using the Clausius–Clapeyron equation from isotherms obtained when reversibility conditions were not respected.

Direct calorimetric measurements also permit the detection of possible modification in the solid. Several phenomena may occur during the sorption, such as breaking of preexisting bonds,[36] induced plasticization with partial crystallization of the polymer,[37] or expansion of the macromolecular chains with large volume changes, to name just a few. In the latter case, where the expansion mechanism is not that described by Flory's model for polymeric gels, the data may be interpreted quite erroneously if the enthalpies and free energies of expansion,[38,39] or the pressure exerted by the polymeric phase because of that expansion,[40] are not taken into account.

Application to Ionomers

The measurement of the energy of hydration will probably provide information on many still unanswered questions about ionomers, particularly regarding the existence of phase separation in the anhydrous state and the swelling conditions of the clusters during hydration. Such measurements were made under suitable conditions for the Nafion perfluorosulfonate membranes which are characterized by a high water diffusion coefficient and a high hydration capacity. These measurements have shown the existence of two stages of hydration for a totally dehydrated sample: below 4–5 H_2O/SO_3^-, the interaction energy is constant and characteristic of the cation: -13 kcal·mol^{-1} for Fe^{++}, -11.5 for H^+, -9.5 for Na^+, and -8.5 for Cu^{++}. These energies essentially follow the order of hydration energies of the cations in loose matrices like clays and thus suggest the existence of an essentially ionic zone in the anhydrous state. Above 4–5 H_2O sulfonate group, the thermal effect decreases measurably and the molar sorption energy approaches zero, which indicates the intervention of an endothermic phenomenon due to the expansion of the cluster. Studies of Nafions at the microscopic or molecular level confirm the existence of these two stages of hydration.[41–43]

Starting Materials, Sample Preparation, and Gravimetry

The copolymers were synthesized by free-radical polymerization of styrene and methacrylic acid (MAA) in the bulk. Several mixtures of different monomer ratios were prepared to obtain polymers of various MAA content. The polymerization was carried out in sealed glass ampoules at 80°C for 18 h, to achieve about 10% conversion. The reaction was then stopped by cooling the ampoules and the polymer was precipitated in methanol. The MAA content was determined by titration of a 5% solution of the polymer in benzene/methanol (90/10, v/v) with methanolic NaOH, to the phenolphtalein end point. The MAA con-

tents of the different polymers were found to be 3.85%, 6.47, 8.8, and 15.9 mol %.

The salt forms used in these experiments were obtained by addition of the exact amount of methanolic NaOH necessary to neutralize completely the methacrylic acid units of polymers of known MAA content. In this way, contamination by phenolphtalein was avoided. The solutions were then freeze-dried to give lightly compacted powdery polymers.

The freeze-dried samples were dried under vacuum at 20°C above T_g. They were then compression molded at 1.4×10^8 N/m^2 at 20°C above the softening point. The resulting disc was removed from the mold while still hot. The experiments below were done on a 15.9% film.

The bulk samples were prepared from freeze-dried material. For each sample, about 0.3–1.8 g polymer were compression molded into a disc about 2 cm in diameter (the larger samples were necessary for the lower ion contents to permit detection of the smaller amounts of water absorbed by these materials). These discs were then remolded but this time between metal plates to obtain larger, thinner samples, the thickness ranging from 0.25 to 0.35 mm. These samples were dried under vacuum and their weight recorded.

The rate of absorption for the bulk samples was measured by immersing the samples in distilled water and recording their weight periodically; the weight was determined by removing the samples from the water, wiping them dry, and weighing them. For the sake of convenience, a brief tabulation is given below listing the weight percent of water corresponding to 1 water molecule per carboxylate group for each of the samples studied in both acid and salt forms.

Molar concentrations	3.85%	6.47%	8.8%	15.9%
1 H_2O/COOH	0.671%	1.132%	1.546%	
1 H_2O/COONa	0.665%	1.117%	1.518%	2.735%

RESULTS

The sorption isotherms for the freeze-dried powdery samples, at 20°C are shown in Figures 1–3 (salt forms), 4–6 (acid forms), and 7 (polystyrene). The equilibrium conditions during the pressure increments were within acceptable limits for all the samples. Before heating, the equilibrium was reached in less than 2 h for small partial pressures and in less than 10 h near the saturation pressure. After heating, a general decrease in the rate of diffusion of water is observed, but it seems unlikely that major errors in the equilibrium data are due to the kinetic parameters only. An example of the kinetic data is plotted in Figure 8 for the 8.8 mol % salt sample.

The sorption isotherm of the 15.9 mol % salt film is not shown, but the hydration data at saturation pressure before and after heating at 180°C are plotted in Figure 9. It seems to take 60 h for the initial sample to reach equilibrium while the absorption is not yet complete in the same time for the sample heated under vacuum.

Tables I and II give a compilation of these data and list several additional factors for each sample, both before and after heating. These additional factors are the total hydration capacity at 20°C at the saturation pressure (line 1), the

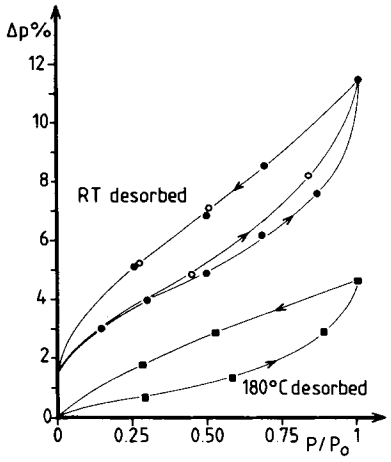

Fig. 1. Sorption isotherm at room temperature for the 8.8% salt form—freeze-dried sample: (●) first run after room temperature desorption; (○) second run after long-time equilibration at saturation pressure and subsequent desorption; (■) after 180°C desorption and subsequent desorption.

fraction of nondesorbable water under vacuum of 10^{-4} torr at 20°C (line 2), and the fraction of sorption at 20°C (line 3).

The sorption at 20°C includes adsorption effects, especially for the freeze-dried samples, due to their very dispersed texture, together with effects associated with the water-ionomer interaction. These two effects may be distinguished (line 4) and expressed in terms of the number of water molecules per dipole (line 5) after subtraction of the hydration data for the pure polystyrene sample which has the same textural characteristics as the freeze-dried copolymers (1.6% before heating and 0.8% after heating, according to Fig. 7). It thus seems that the 6.5%

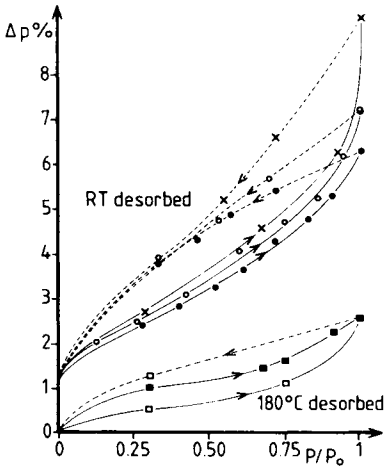

Fig. 2. Sorption isotherm at room temperature for the 6.47% salt form—freeze-dried sample: (●) first run after room temperature desorption; (○) second run after long-time equilibration at saturation pressure and subsequent desorption; (x) third run after soaking in liquid water and subsequent desorption; (□) first run after 180°C desorption; (■) second run after long-time equilibration at saturation pressure and subsequent desorption.

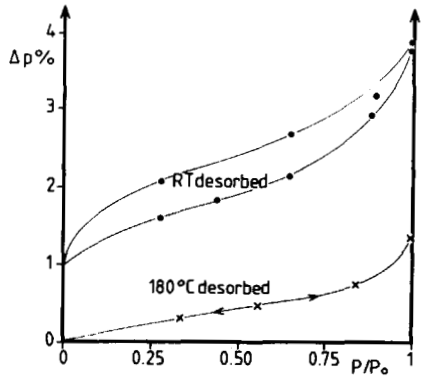

Fig. 3. Sorption isotherm at room temperature for the 3.85% salt form—freeze-dried sample: (●) after room temperature desorption; (X) after 180°C desorption.

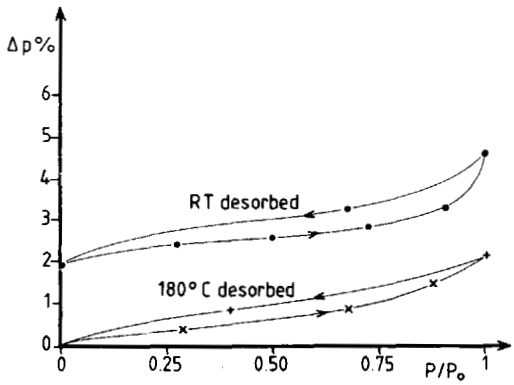

Fig. 4. Sorption isotherm at room temperature for the 8.8% acid form—freeze-dried sample: (●) after RT desorption; (X) after 180°C desorption.

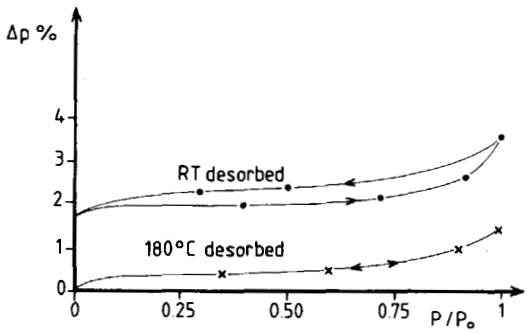

Fig. 5. Sorption isotherm at RT for the 6.47% acid form—freeze-dried sample: (●) after RT desorption; (X) after 180°C desorption.

and the 8.8% samples are the only ones exhibiting a large enough water sorption as compared to the textural effects, to allow the evaluation of the interaction energy by microcalorimetry to be approximately representative of the ionic water–dipole interaction. The energy profiles for these two samples are plotted

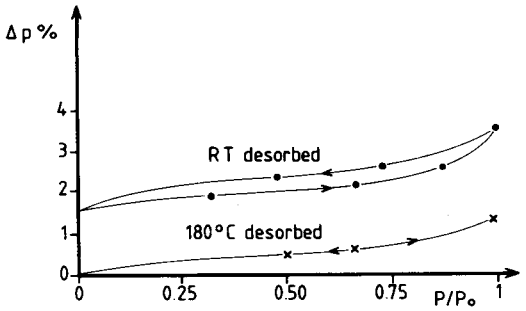

Fig. 6. Sorption isotherm at RT for the 3.85% acid form, freeze-dried sample: (●) after RT desorption; (x) after 180°C desorption.

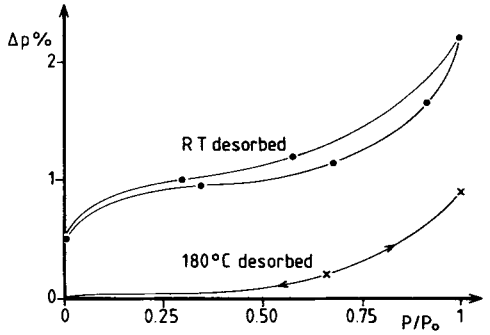

Fig. 7. Sorption isotherm at RT for the freeze-dried polystyrene: (●) after RT desorption; (x) after 180°C desorption.

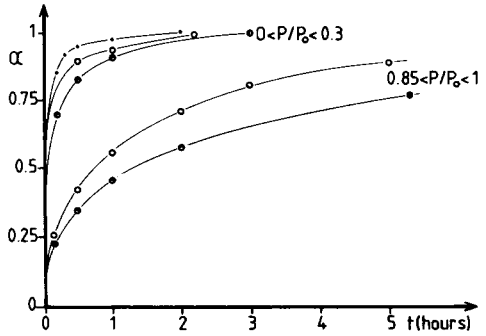

Fig. 8. Kinetics of absorption at RT for the 8.8% salt form, freeze-dried sample: (●) RT desorbed; (○) after liquid water soaking; (⊙) 180°C desorbed.

in Figures 10 and 11 [the reported water content corresponding to the total sorption measured experimentally (line 3)].

The nondesorbable water still present under 10^{-4} torr at 20°C is eliminated by heating the sample under vacuum from 20°C to 180°C. The results obtained for a linear temperature increase are plotted in Figures 12 and 13. The samples are heated at 180°C until constant weight is reached. Table III shows that after subtraction of the weight lost by pure polystyrene under the same heating con-

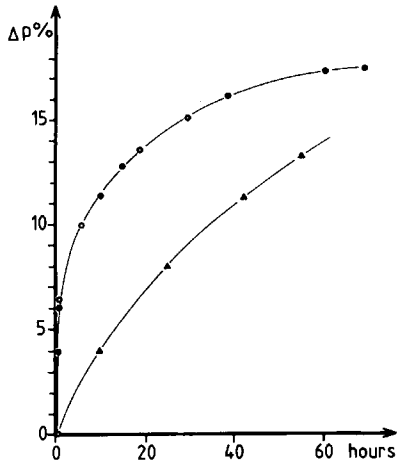

Fig. 9. Sorption curves at 20°C for the 15.9% salt form, 0.3 mm thick film: (●) as received; (○) after annealing at 180°C and cooling under water pressure; (△) after annealing at 180°C and cooling under vacuum.

ditions (0.5%), the amount of residual water at room temperature is a little less than 1 H_2O per dipole for the freeze-dried samples and above this value for the film.

Bulk absorptions for three temperatures (room temperature, 45°C, 70°C) are shown in Figures 14, 15, and 16, respectively. Data are presented on a log–log plot for the sake of convenience rather than for theoretical reasons. It is noteworthy that none of the curves show an equilibrium absorption within the time scale of the measurements (more than 1 year). It should also be pointed out that some of the samples showed a slight thickening in a few regions reminescent of blister formation. However, the general shapes of the curves did not seem to depend on whether blisters formed or not.

In an attempts to see whether the freeze-dried powdery PS also exhibited long

TABLE I
Salt Forms

Molar concentration	3.85%	6.47%	8.8%	15.9% film
Before heating				
1. Total hydration capacity at 20°C	4	9	11.5	17.25
2. Nondesorbable water at 20°C	1.05	1.16	1.5	3.95
3. Reversible desorbable water at 20°C	2.95	7.84	10	14.3
4. Reversible desorbable water at 20°C after subtraction of the adsorption due to the texture	1.35	6.24	8.4	
5. Number of water molecules per dipole	2	5.6	5.5	5.22
After heating				
1. Total hydration capacity at 20°C	1.35	2.6	4.5	>14
2. Nondesorbable water at 20°C	0	0	0	2.7
3. Reversible desorbable water at 20°C	1.35	2.6	4.5	
4. Reversible desorbable water at 20°C after subtraction of the adsorption due to the texture	0.55	1.8	3.7	
5. Number of water molecules per dipole	0.8	1.6	2.4	>4.1

TABLE II
Acid Forms

Molar concentration	3.85%	6.47%	8.8%
Before heating			
1. Total hydration capacity at 20°C	3.4	3.5	4.7
2. Nondesorbable water at 20°C	1.5	1.6	1.9
3. Reversible desorbable water at 20°C	1.9	1.9	2.8
4. Reversible desorbable water at 20°C after subtraction of the adsorption due to the texture	0.3	0.3	1.2
5. Number of water molecules per dipole	0.45	0.3	0.8
After heating			
1. Total hydration capacity at 20°C	1.3	1.3	2.1
2. Nondesorbable water at 20°C	0	0	0
3. Reversible desorbable water at 20°C	1.3	1.3	2.1
4. Reversible desorbable water at 20°C after subtraction of the adsorption due to the texture	0.5	0.5	1.3
5. Number of water molecules per dipole	0.7	0.5	0.8

TABLE III

	Freeze-dried samples						Film,
	Salt forms			Acid forms			salt form
Molar conc	3.85%	6.47%	8.8%	3.85%	6.47%	8.8%	15.9%
Desorption by heating	1.05	1.16	1.56	1.4	1.5	1.8	3.85
After correction	0.05	0.66	1.06		1	1.3	
Number of H_2O per dipole	0.8	0.6	0.7		0.88	.085	1.44

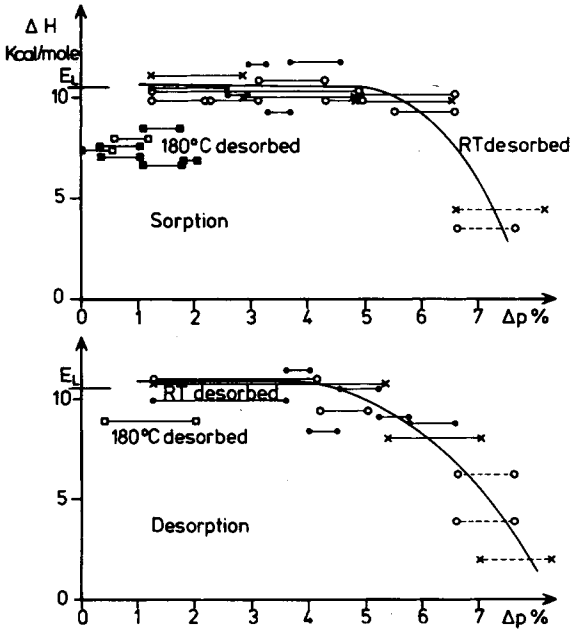

Fig. 10. Energy profiles during sorption and desorption for the 6.47% salt form, freeze-dried sample. (●) First sorption; (○) second sorption; (×) third sorption.

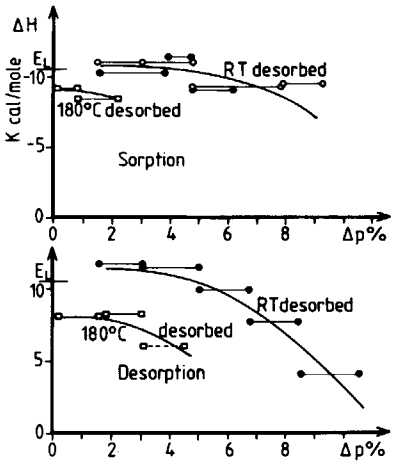

Fig. 11. Energy profiles during sorption and desorption for the 8.8% salt form, freeze-dried sample. Average value of the molar energy during the increment: (●) after RT desorption; (○) after long-time equilibration at saturation and subsequent desorption; (□) after 180°C desorption.

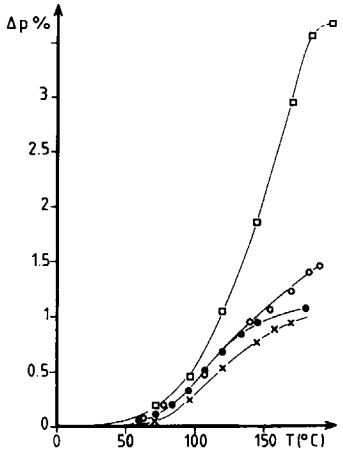

Fig. 12. Amount of water desorbed when sample is heated under vacuum (10^{-4} torr) from room temperature to 180°C, salt form: (□) 15.9% (film); (○) 8.8%; (●) 6.47%; (x) 3.85%.

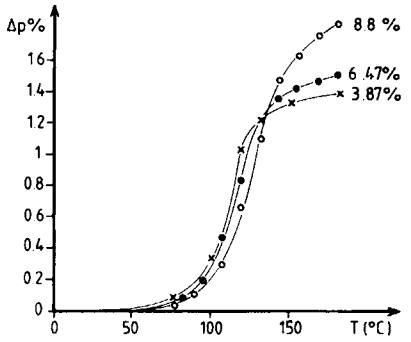

Fig. 13. Amount of water desorbed when sample is heated under vacuum (10^{-4} torr) from room temperature to 180°C, acid form.

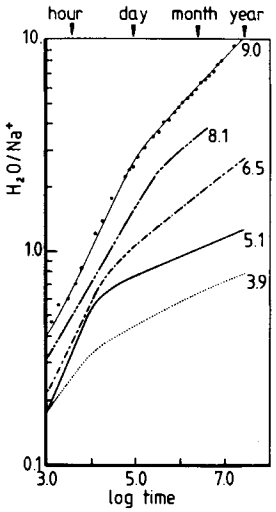

Fig. 14. Water absorption as a function of time at room temperature, for ~0.3 mm thick samples.

term effects of the type observed for the samples of ca. 0.3 mm thickness, long term (>100 h) absorption experiments were performed on the powdery materials also. The results showed clearly that there is no long term effects in the powdery samples since the weight vs. time curves were absolutely flat.

DISCUSSION

From the preceeding results, several conclusions can be drawn concerning the effects of the preparation conditions, the concentration in ionic groups and the thermal history on the hydration of the ionic aggregates.

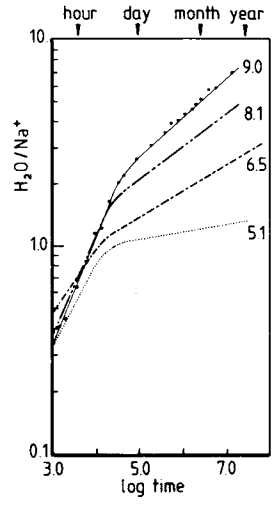

Fig. 15. Water absorption as a function of time at 45°C, for ~0.3 mm thick samples.

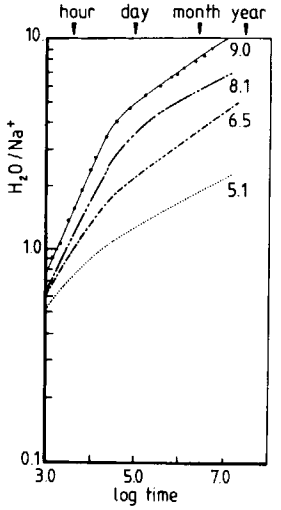

Fig. 16. Water absorption as a function of time at 70°C, for ~0.3 mm thick samples.

The first result of these experiments shows that the freeze-dried acid and salt samples exhibit major differences in their hydration capacities. Furthermore, for the salt samples, the hydration capacity also changes with the ion concentration. These samples thus seem to be representative of the ionic association phenomenon responsible for the supermolecular structures of ionomers deduced from their mechanical and viscoelastic properties, as well as from the diffraction data. Some features of this structure are probably established during the preparation of the copolymers in the glassy state, even before the samples are dried and molded above T_g.

Influence of the Nature and the Concentration of Ionic Groups on the Hydration Capacity. An examination of Tables I and II (line 5) shows that the hydration capacity of the powder acids stays below 1 H_2O per COOH for all methacrylic acid concentrations. For the powder salts, however, one finds 2 H_2O/COONa for the 3.85% sample and the value stays constant at about 5 H_2O COONa for all the other percentages, including the 15.9% thin film. The constant hydration capacity per COONa group within the phase-separated regions is not easily explained since all the aggregates are not located in a single phase. The hydration capacity therefore does not seem to depend on the nature of the phase.

From Raman studies it is known that in this ion content region, the concentration of multiplets remains the same, while the total number of ions in the clustered phase increases with ion concentration. One possible interpretation of the results might be that both the multiplets and the clusters have a constant hydration capacity of 5–6 H_2O molecules/COONa group, independent of their environment. Another explanation, which is consistent with the rate of water absorption by the bulk samples, might be that it is only the multiplets which are hydrated rapidly, while water absorption into the clusters requires very much longer time periods (months to years in bulks samples as shown in Figures 14–16). On the other hand, if it is primarily the multiplets which absorb the water over the short-time scale, the absorption capacity of these species would have to be

extremely high. Another possibility is that multiplets in the matrix as well as multiplets in the clusters are hydrated rapidly, but that there is afterwards a transformation of the cluster structure which allows a further hydration of these species. An alternate possibility for the behavior will be offered later.

Hydration Energies. At low partial pressures, the average molar hydration energies do not vary appreciably with ion content, being ca. -10.5 kcal·mol^{-1} for the powder salts and about -9 kcal·mol^{-1} for the acids. It can simply be said that the interactions between water and the ionic aggregates are of about the same order of magnitude in terms of energy as the water–water interactions in the liquid phase, whereas the interactions between water and the acid dimers seem somewhat weaker. The acids and the salts behave quite differently at high partial pressures. For the acids, the fraction of the adsorption due to the expanded texture is predominant and the average molar energy, even though measured under very imprecise conditions, seems to be in the neighborhood of the liquefaction energy of water (10 kcal·mol^{-1}). For the salts, the sorption accounts for a significant fraction of the process, and the energy profiles in Figures 10 and 11 show that above a certain water content (4 H_2O/COONa after corrections for surface effects), the average energy becomes much lower than the liquefaction energy, indicating the intervention of an endothermic term reflecting the change in volume necessary for the expansion of the clusters. This is similar to the results obtained for Nafions. This type of energetic behavior during the hydration process thus seems to be characteristic of phase separation between ionic aggregates and essentially organic regions. The reason for this behavior might be the following: since the clusters are relatively large and contain a considerable amount of organic material, it is conceivable that, for a water molecule to enter the cluster, the organic chain molecules would have to be rearranged over distances involving a number of segments. Such viscoelastic processes would be expected to be exceedingly slow in bulk samples at temperatures significantly below the T_g of polystyrene (ca. 100°C) or the softening point of the dry clusters (150–200°C depending on total ion content), although they might be quite rapid in powdery samples.

It should be noted that the water content of 4 H_2O/COONa at which the interaction energy starts to decrease is exceeded only after many successive cycles and especially by soaking the samples in liquid water. The proposed interpretation is that water plasticizes the polymers, and, in the freeze-dried samples, permits an expansion of the sample. After desorption, however, the chains are not able to go back to their original shape, since the samples are below their glass transition temperature; the osmotic pressure during subsequent sorptions is thus much lower, which would account for the regular shift of the whole isotherm toward higher water contents. This phenomenon is not found in the film, but it should be interesting to find out if much longer times might not modify the equilibria apparently established in less than 100 h.

Influence of the Thermal History. Annealing above T_g under vacuum achieves complete dehydration with an average loss of 1 H_2O/COO^-. Contrary to the Nafions, the 20°C hydration properties are not reestablished. They stay very different even after numerous sorption-desorption cycles or after prolonged soaking in liquid water (more than 15 days). The results are shown in Tables I and II. It is interesting to note the disappearance, for the acids, of the nondesorbable water at room temperature under vacuum; the desorbable sorption at 20°C however, remains unchanged, with a value of less than 1 H_2O/COOH.

The nondesorbable water also disappears for the salt forms, but the desorbable sorption is noticeably lower than that of the initial samples. As can be seen in Table I (line 5), the hydration capacity increases regularly with the molar concentration of ions; the value of 5 H_2O/COONa, which reflects the presence of clusters as well as the presence of nondesorbable water, is recovered only above 15 mol % of ions. An experiment was performed using a 7.7 mol % thin film: the results fell exactly on the curve, between the 6.47 and 8.8 mol % freeze-dried samples. The behavior after heating seems independent of the texture or the preparation conditions.

Energetically, Figures 10 and 11 show that the molar interaction energy is lower with a value of about -9 kcal·mol^{-1} instead of -10.5. Thus, annealing above T_g, which is accompanied by total dehydration, modifies the supermolecular structures due to ionic association. In particular, phase separation characteristics are observed only when the ionic concentration is considerably higher than 6%. Surprisingly, the supermolecular structure was determined from the properties of films obtained from freeze-dried samples which were dehydrated under vacuum at 140°C and compression molded above 200°C. This may be explained, however, by the fact that the samples were removed from the mold at high temperatures but cooled in the ambient atmosphere and thus in the presence of water vapor. As can be seen in Figure 9, cooling from 180°C to 20°C in the presence of partial pressures of water vapor restores the initial hydration properties of the film.

The thermal history of the samples is thus influenced by the presence of water vapor. The supermolecular structure is modified through total dehydration: in particular, the 6% critical concentration disappears and the phase separation characteristics, as far as hydration is concerned, reappear only at higher molar ionic concentrations. Important conclusions may be drawn concerning the influence of water on the flow and relaxation properties of these materials.

Influence of Sample Dimensions. The results obtained in these experiments show the influence of the sample dimensions on the long-term absorption phenomena of this polymeric system. The kinetics are fast for the powdered material, and equilibrium is attained quite rapidly. With the 0.3 mm thick films, equilibrium has not yet been reached after soaking in water for 1 year; the samples of high ion content become opaque suggesting the presence of large scattering centers which are probably water clusters. The clustering of water molecules in polymers has been observed before.[27] In these samples, the driving force for absorption thus seems large enough to accomplish rheological work, i.e., to push the chains apart and create water-filled regions in the matrix. With the very thick samples,[12] equilibrium is not attained within less than 1 year, probably because the driving force is not great enough to accomplish extensive rheological work. Finally, it is worth noting that no evidence for case II diffusion[44–46] was found in these materials.

Thus, it seems likely that some type of short-term equilibrium is attained quite rapidly for all samples. However, in those samples in which rheological work can be done by the excess hydration energy, major changes in the cluster geometries are achieved over periods of 1 year. This may involve formation of water-filled clusters of the type encountered in the Nafions.

Two of us (A. E. and S. G.) are indebted to the U. S. Army Research Office for partial financial support of this research. It is also a pleasure to acknowledge the assistance of Drs. Kazuo Arai and Mitsuaki Hashiyama in the early stages of the water uptake determination of the disc samples.

APPENDIX: THERMODYNAMIC EVALUATION OF THE CALORIMETRIC MEASUREMENTS

Adsorption Microcalorimetry in Inert Solids

The heats measured in kcal·mol^{-1} should be expressed in terms of thermodynamic values. Because the experimental conditions enter into consideration, this is not always a trivial task. The measurements made using the present experimental assembly corresponded to calorimetric isothermal adsorption measurements in an open system. For an infinitesimal change, the initial and final states may be characterized by Table IV.

From the first law of thermodynamics (energy conservation) the variation of the initial total internal energy of the system expressed as $d(n_g e_g + n_a e_a)$ may be considered to be the sum of the energy the system received from outside, i.e., the work dW, and an amount of heat dQ measured experimentally, plus the energy associated with the $(dn_g + dn_a)$ mol of gas having an energy e_g as they enter the system:

$$d(n_g e_g + n_a e_a) = dw + dQ_{\text{expt}} + e_g(dn_g + dn_a)$$

$$dQ_{\text{expt}} = (e_a - e_g)\, dn_A + n_a\, de_a - dw$$

The work dW done on the system may be expressed as $P\,dV$ and $P\,dV = RT(dn_g + dn_A)$. However, $RT\,dn_g = V_g$ dP, and this term is calibrated directly under exactly the same conditions as those prevailing during the experiments but in the absence of adsorbent. The calculations in terms of kcal·mol^{-1} are always done after this correction has been applied; this correction becomes important especially around the saturating pressure which again limits the validity of the measurements at this level. The final expression is then

$$\frac{dQ_{\text{corr}}}{dn_a} = e_a - e_g + n_a \frac{de_a}{dn_a} - RT$$

where the molar integral adsorption energy is $g_i = e_a - e_g$ and the molar differential adsorption energy is

$$q_d = e_a - \frac{e_g + n_a\, de_a}{dn_a}$$

Furthermore, the isosteric heat is calculated from the Clausius–Clapeyron equation, $q_{st} = -RT^2 (\partial \ln P/\partial T)_{n_a}$ from isosteres $P = f(T)$ at constant n_a. The thermodynamic expression is

$$q_{st} = e_a - e_g + n_a \frac{de_a}{dn_a} - RT$$

Thus, the measured molar heat, after correction for the term related to the instrument, is the isosteric heat, or, ignoring the RT term, the molar differential heat of adsorption.

In reality, however, the experimental measurements do not correspond to infinitesimal transformations. The integrated expression should thus be used

$$\frac{\Delta Q_{\text{corr}}}{\Delta n_a} = \frac{\Delta[n_a(e_a - e_g)]}{\Delta n_a} - RT$$

The calorimetric measurements during a partial pressure increment correspond, in effect, to the variation in the integral heat of sorption normalized to 1 mol. It can be considered as the variation

TABLE IV

	Initial state	Final state
Temperature	T	T
Equilibrium pressure	P	$P + dP$
Volume of the gas	V_g	V_g
Number of moles of gas	n_j	$n_j + dn_j$
Number of moles adsorbed	n_a	$n_a + dn_a$
Molar internal energy of gas	e_g	e_g
Molar internal energy of the absorbed phase	e_a	$e_a + dn_a$

in the internal energy of 1 mol *absorbed during this increment;* it is not the average molar energy of all the moles adsorbed so far. Successive calorimetric measurements during an isotherm allow the determination of the energy profile of the sorption and the detection of changes in the nature of the interactions.

It should be emphasized that the thermodynamic values directly accessible by calorimetry are the internal energies. To obtain the enthalpies ($H = E + PV$), the measurements should be done at constant pressure, which means at constant surface pressure ϕ for the adsorbed phase. These conditions cannot be attained with microcalorimetric instrumentation but the work done by this expansion pressure may be evaluated through calculations and the average molar enthalpy h_a of the adsorption layer determined from calorimetric measurements using the following expression:

$$\frac{\Delta Q}{\Delta n_a} = h_g - h_a + \phi\frac{A}{n_a}$$

This equation is often extended to calculate the average molar entropy of the adsorbate S_a, which is the thermodynamic value most characteristic of the state of the adsorbed film. Taking the entropy of water S_L at the saturating pressure P_0 as a reference state,

$$\frac{\Delta Q}{\Delta n_a} = T(S_L - S_a) + \Lambda - RT\ln\frac{P_0}{P} + \phi\frac{A}{n_a}$$

where Λ is the latent energy of condensation.

Sorption Microcalorimetry for Noninert Solids

In all the above expressions, it is assumed that the only participation of the solid is in creating the force field in which the adsorbed phase is immersed. If this is not the case, the calorimetric measurements also reflect the variation in the internal energy of the system.

This is particularly important in the case of polymer–solvent interactions where diffusion and dissolution processes may cause significant modifications in the solid phase.

References

1. L. Holliday, *Ionic Polymers*, Halstead, Wiley, New York, 1975.
2. A. Eisenberg and M. King, "Ion Containing Polymers, Physical Properties and Structures," in *Polymer Physics*, R. S. Stein, Ed., Vol. 2, Academic Press. New York, 1977.
3. A. Eisenberg, *Ions in Polymers*, in Advances in Chemistry Series **187,** American Chemical Society, Washington, D.C., 1980.
4. T. C. Ward and A. V. Tobolsky, *J. Appl. Polym. Sci.*, **11,** 2403 (1967).
5. E. P. Otocka and T. K. Kwei, *Macromolecules*, **1,** 401 (1968).
6. R. Longworth, in *Ionic Polymers*, L. Holliday, Ed., Halstead, Wiley, New York, 1975, Chap. 2.
7. W. J. MacKnight, *Macromol. Rev.*, **16,** 41 (1981).
8. C. L. Marx and S. L. Cooper, *J. Macromol. Sci.*, **B9,** 19 (1974).
9. W. E. Fitzgerald and L. E. Nielson, *Proc. Roy. Soc. (London)*, **A282,** 137 (1964).
10. N. Z. Erdi and H. Morawitz, *J. Colloid. Sci.*, **19,** 708, (1964).
11. A. Eisenberg and M. Navratil, *J. Polym. Sci., Polym. Lett. Ed.*, **10,** 537 (1972).
12. A. Eisenberg and M. Navratil, *Macromolecules*, **6,** 604 (1973).
13. N. Brockman and A. Eisenberg, *Polym. Prepr.*, **22,** 355 (1981).
14. S. Gauthier and A. Eisenberg, *Polym. Prepr.*, **22,** 293 (1981).
15. M. Rigdahl and A. Eisenberg, *J. Polym. Sci., Polym. Phys. Ed.*, **19,** 1641 (1981).
16. R. D. Lundberg and H. S. Makowski, *Ions in Polymers*, Advances in Chemistry Series **187,** American Chemical Society, Washington, D.C., 1980, p. 21.
17. E. P. Otocka and F. R. Eirich, *J. Polym. Sci., A-2,* **6,** 921 (1968).
18. E. P. Otocka and F. R. Eirich, *J. Polym. Sci., A-2,* **6,** 933 (1968).
19. M. Pineri, C. Meyer, A. M. Levelut, and M. Lambert, *J. Polym. Sci., Polym. Phys. Ed.*, **12,** 115 (1974).
20. H. S. Makowski, R. D. Lundberg, L. Westerman, and J. Bock, *Ions in Polymers*, Advances in Chemistry Series **187,** American Chemical Society, Washington, D.C., 1980, p. 3.

21. D. Brenner and A. A. Oswald, *Ions in Polymers*, Advances in Chemistry Series **187,** American Chemical Society, Washington, D.C., 1980, p. 53.
22. A. Eisenberg, H. Matsuura, and T. Tsutsui, *J. Polym. Sci., Polym. Phys. Ed.*, **18,** 479 (1980).
23. D. Rahrig and W. J. MacKnight, *Ions in Polymers*, Advances in Chemistry Series **187,** American Chemical Society, Washington, D.C., 1980, p. 77.
24. D. Rahrig and W. J. MacKnight, *Ions in Polymers*, Advances in Chemistry Series **187,** American Chemical Society, Washington, D.C., 1980, p. 91.
25. A. Eisenberg and H. Yeager, Eds., *Perfluorinated Ionomer Membranes*, ACS Symposium Series, American Chemical Society, Washington, D.C., 1982, to appear.
26. A. Eisenberg and M. Navratil, *Macromolecules*, **7,** 90 (1974).
27. H. W. Starkweather, Jr., *Structure Solubility Relationships in Polymers*, F. W. Harris and R. B. Seymour Eds., Academic, New York, 1977.
28. A. Nepel, I. S. Butler, and A. Eisenberg, *J. Polym. Sci., Polym. Phys. Ed.*, **17,** 2145 (1979).
29. M. Pineri, R. Duplessix, S. Gauthier, and A. Eisenberg, *Ions in Polymers*, Advances in Chemistry Series **187,** American Chemical Society, Washington, D.C., 1980, p. 283.
30. M. Escoubes, J. F. Quinson, J. Gielly, and M. Murat, *Bull. Soc. Chim. Fr.*, **5,** 1689 (1972).
31. Cl. Letoquart, Fr. Rouquerol, and J. Rouquerol, *J. Chim. Phys.* **3,** 559 (1973).
32. P. Chiche, *J. Chim. Phys.*, **49,** 375 (1962).
33. M. H. Pineri, M. Escoubes, and E. Roche, *Biopolymers*, **17**(12), 2799 (1978).
34. C. A. J. Hoeve, *Am. Chem. Soc. Symp. Ser.*, **127,** 135 (1980).
35. J. A. Rupley, P. H. Yang, and G. Tollin, *Am. Chem. Soc. Sympos. Ser.*, **127,** 111 (1980).
36. J. Guillet, G. Seytre, A. Douillard, and M. Escoubes, *Angew. Makromol. Chem.*, **68,** 149–162 (1978).
37. M. Escoubes, D. Moser, and P. Berticat, *Angew. Makromol. Chem.* **67,** 991, 45–60 (1978).
38. H. J. C. Berendsen, *Water in Disperse Systems*, F. Franks, Ed., Plenum, New York, 1975, Vol. 5, p. 293.
39. M. Brener, E. M. Buras, Jr., and A. Fookson, *Am. Chem. Soc. Symp. Ser.*, **127,** 311 (1981).
40. H. W. Starkweather, *Am. Chem. Soc. Symp. Ser.*, **127,** 433 (1981).
41. E. Southern, A. C. Thomas, *Am. Chem. Soc., Symp. Ser.*, **127,** 375 (1980).
42. R. Duplessix, M. Escoubes, B. Rodmacq, F. Volino, E. Roche, A. Eisenberg, and M. Pineri, *Am. Chem. Soc. Symp. Ser.*, **127,** 470–486 (1980).
43. B. Rodmacq, J. M. Coly, M. Escoubes, E. Roche, R. Duplessix, A. Eisenberg, and M. Pineri, *Am. Chem. Soc. Symp. Ser.* **127,** 487–501 (1980).
44. T. Alfrey, E. F. Gurner, and W. G. Lloyd, *J. Polym. Sci. C*, **12,** 249 (1966).
45. G. C. Sarte, *Polymer*, **20,** 827, (1979).
46. N. L. Thomas and A. H. Windle, *Polymer*, **23,** 1982, to appear.

Received February 18, 1983
Accepted October 31, 1983